Progress in Additive Manufacturing
https://doi.org/10.1007/s40964-026-01624-9

RESEARCH

Evaluation of machinability and surface quality enhancement of material extrusion fabricated polylactic acid cylinders through lathe machining parameters

Fermin Bañon-Garcia[1] · Sergio Martin-Bejar[1] · Carolina Bermudo[1] · Francisco Javier Trujillo[1] · Lorenzo Sevilla[1]

Received: 12 January 2026 / Accepted: 25 February 2026

Abstract

This study examines the effect of lathe machining parameters on the machinability and surface quality of polylactic acid (PLA) cylinders produced using material extrusion technology. The research focuses on the correlation between cutting parameters, machining temperature, and factors such as required machining force and associated power consumption. The aim is to improve the final product quality while reducing production times. The comparison between high-quality, time-intensive printed pieces and normally printed pieces complemented by a post-machining operation shows that incorporating a machining step significantly improves surface quality and operational efficiency. The critical examination of the machining temperature, which is essential due to the thermoplastic nature of PLA and its low glass transition temperature, highlighted the influence of cutting speed and feed rate. Overall, feed rate was identified as the dominant parameter controlling mechanical loading and surface roughness, whereas cutting speed primarily governed thermal response and instantaneous power demand. The integrated analysis supports a process window in which compressed air assistance mitigates heat accumulation and promotes stable chip evacuation. From a manufacturing perspective, printing at a productive layer height followed by a short turning operation provides a competitive route to achieve high quality rotational surfaces compared with fine layer FFF printing, particularly for batch production.

Highlights

- Compressed air lowers cutting temps and improves surface quality.
- Post-FFF turning enhances PLA surfaces vs. 0.1 mm layer parts.
- Cutting parameters optimize PLA machining and cut process time.
- Speed and feed changes boost quality and efficiency vs. 0.1 mm parts.

Keywords Material extrusion technology · Turning · Machinability · Machining · PLA

1 Introduction

Additive manufacturing (AM) has changed the way complex products are produced, enabling the creation of parts that were previously difficult or impossible to manufacture using traditional methods [1]. This technology is particularly useful in sectors such as aeronautics, automotive and construction, where it can offer customised and efficient solutions [2].

However, Fused Filament Fabrication (FFF), also known as fused deposition modeling or filament freeform fabrication, additive manufacturing faces challenges, especially in terms of production times and the surface quality of the

✉ Fermin Bañon-Garcia
fermin.banon@uma.es

Sergio Martin-Bejar
smartinb@uma.es

Carolina Bermudo
bgamboa@uma.es

Francisco Javier Trujillo
trujillov@uma.es

Lorenzo Sevilla
lsevilla@uma.es

[1] Department of Civil, Materials and Manufacturing Engineering, University of Malaga, Malaga 29071, Spain

Published online: 23 March 2026

parts [3]. This is a problem for industries that require tight tolerances and quality surface finishes [4]. The FFF process does not always meet these expectations due to its limited surface finish and production speed [5]. Layer resolution and accuracy are limited by the layer-by-layer construction technique and filament size, which can lead to unevenly textured surfaces, especially in curves [6]. The thermoplastic materials used vary in properties, affecting the uniformity and dimensional accuracy of the finish [7–9]. Production speed, although fast, must be balanced with the need for precision and quality, as increasing speed can result in defects such as warping and adhesion problems [10]. In addition, the supports and post-processing required for certain geometries increase production time and cost, requiring manual labour and additional techniques to improve the surface finish [11, 12].

To improve the quality of the final parts and to meet efficiency requirements, it is necessary to consider secondary operations [13, 14]. Grinding, polishing and coating can significantly improve the surface quality of parts created with FFF, while techniques such as CNC (Computer Numerical Control) machining help to correct dimensional accuracy problems caused by material shrinkage, deformation and inaccuracies in filament deposition [15–17]. In addition, these post-printing processes can optimise the mechanical properties of the parts by strengthening the bonds between layers [18–20].

Within these secondary operations, a turning process stands out as a beneficial post-FFF machining operation due to the high number of revolution parts in the industry, which can help overcome the limitations of additive manufacturing. This process allows for the correction and optimisation of part dimensions to meet specific requirements, improving dimensional accuracy and functionality [21]. In addition, turning can significantly improve surface finish, eliminating the layer texture characteristic of FFF and providing smooth, uniform surfaces, essential in applications where appearance and reduced flow resistance are critical [22]. In combination, integrating turning speeds production time by enabling faster and more effective material removal compared to achieving a similar finish with FFF alone. Additionally, the turning process can benefit the mechanical properties of machined parts, align surface stresses and improving strength in structural or load-bearing applications [23].

However, assessing how thermoplastic materials used in FFF, such as PLA, can be machined presents challenges. Yang et al. [22] have evaluated the machinability of thermoplastic materials such as PEEK, PI and PMMA, finding significant differences in the response of each material under various machining conditions, indicating the need to adjust the parameters for each polymer. These materials have particular thermal and mechanical properties that complicate machining [24]. Cutting parameters when machining PLA are important, with machining temperature being a critical factor to consider. Masek et al. [25] demonstrates the effectiveness of using tool-to-workpiece thermocouples to measure temperature in the turning of thermoplastic composites, which helps to optimise cutting parameters and improve machining quality. The low glass transition temperature of thermoplastics, together with the way filaments are stacked during FFF manufacturing, affects the machining result. This aspect makes PLA prone to softening or melting with the heat generated by friction on the lathe, which can compromise the accuracy and surface quality of the part. In addition, this heat can cause warping, especially in thin sections or if the part is not properly clamped. Moreover, the structure of 3D printed parts, characterised by overlapping layers, introduces an anisotropy in their mechanical properties that can lead to unexpected behaviour during machining, such as delamination or breakage [26, 27].

Thus, the correct choice of cutting tools and the optimisation of machining parameters are essential to reduce the heat generated and prevent damage to the workpiece, ensuring an efficient process and quality results [28]. Erenkov et al. [29] explores the use of ceramic cutting tools in thermoplastic turning, which can offer advantages in terms of surface quality and tool life, suggesting that ceramic materials are suitable for these operations.

Recent literature has increasingly addressed post-processing of additively manufactured polymers and hybrid AM–CNC strategies to overcome the characteristic staircase effect and limited dimensional capability of material extrusion. Comprehensive reviews have classified post-processing routes for polymer AM, highlighting the trade-offs between chemical smoothing, mechanical finishing and hybrid sequences in terms of achievable roughness, geometric accessibility and process constraints [30]. For PLA-based systems, post-treatments such as annealing and vapour/solvent approaches can markedly improve surface appearance, although they may compromise dimensional accuracy or mechanical performance depending on the method and material system [4, 31]. Mechanical post-processing alternatives, including burnishing-type approaches, have also demonstrated the potential to improve surface finish without solvent interaction, albeit with geometry-dependent limitations [32]. More recently, hybrid manufacturing concepts integrating in-process machining with fused filament fabrication have been reported as a viable route to combine coarse, productive printing with a rapid finishing pass, thereby improving surface quality while reducing overall cycle time [33]. In this context, the present study contributes an application-oriented machinability perspective for FFF-manufactured PLA, linking temperature

evolution, cutting forces and energy consumption to surface roughness outcomes under controlled turning conditions, thus complementing prior post-processing studies that predominantly focus on surface metrics alone.

Although the influence of cutting parameters on temperature and surface quality has been previously reported for thermoplastic materials, studies addressing the machinability of PLA components manufactured by fused filament fabrication remain limited. In particular, the combined analysis of thermomechanical response, energy consumption, and surface quality during turning of FFF fabricated PLA has not been sufficiently explored. The layered structure and anisotropic behaviour inherent to material extrusion introduce additional challenges compared to conventionally processed polymers, especially when machining near the glass transition temperature. In this context, the present work provides an integrated experimental assessment of cutting temperature, cutting forces, energy consumption, and surface roughness under controlled turning conditions, while also evaluating turning as an industrially viable post processing strategy in hybrid FFF CNC workflows.

Most studies on polymer machining have focused on conventionally processed thermoplastics, where material homogeneity, isotropic mechanical behaviour, and stable thermal properties can be assumed. In contrast, PLA components manufactured by fused filament fabrication exhibit a layered architecture, anisotropic behaviour, interlayer bonding effects, and reduced thermal conductivity, which fundamentally alter their response to cutting operations. Despite the widespread use of FFF for functional PLA parts, the machinability of FFF-fabricated PLA has received comparatively limited attention, and existing works often address post-processing mainly from a surface finish perspective without correlating thermal, mechanical, and energetic responses. As a result, the definition of process windows and mechanistic understanding derived from conventional polymer machining cannot be directly transferred to FFF-manufactured PLA. The present study addresses this gap by providing an integrated machinability assessment specifically focused on turning of FFF-fabricated PLA, linking cutting temperature evolution, cutting forces, energy consumption, and surface roughness under controlled conditions.

Previous studies on thermoplastic machining have reported the influence of cutting parameters on surface roughness, cutting forces, and temperature, mainly focusing on conventionally processed polymers or on isolated post-processing outcomes in additively manufactured parts. For example, the role of thermal softening and viscous deformation in polymer machining has been extensively discussed for bulk thermoplastics, highlighting the sensitivity of cutting behaviour to temperature near the glass transition region [23]. In the context of additively manufactured components, CNC-based post-processing has been primarily analysed from a surface finish perspective, often without correlating thermal, mechanical, and energetic responses under identical conditions [34]. The results obtained in the present work are consistent with these general trends; however, the integrated experimental framework applied here reveals additional insights specific to fused filament fabricated PLA. While cutting speed exhibited a limited direct influence on cutting force magnitudes within the analysed range, its pronounced effect on temperature evolution and energy consumption underscores the dominant role of thermally driven material behaviour in FFF parts, where the layered structure and reduced thermal conductivity further amplify heat accumulation effects. This distinction is not always evident in studies addressing surface quality optimisation alone [35], nor in alternative post-processing approaches such as chemical vapour smoothing, which improve roughness but provide limited control over thermomechanical loading and dimensional accuracy [31].

Despite the increasing adoption of Fused Filament Fabrication for functional polymer components, relatively limited research has examined the machinability of FFF manufactured PLA under controlled turning conditions using an integrated process quality perspective. This study presents a combined experimental assessment of cutting temperature evolution, cutting forces, energy consumption, and surface roughness during turning of material extrusion PLA. Compressed air assisted turning is also evaluated as a practical post processing strategy.

Therefore, this study seeks to optimise the turning process for PLA parts produced by FFF, with the aim of improving the quality of the final product and reducing operating times, while maintaining a focus on how the cutting parameters affect part quality. To achieve high-quality parts with precise tolerances produced through Fused Filament Fabrication (FFF), it is imperative to undertake post-processing operations, such as turning. While there is existing literature on the machining of thermoplastic polymers manufactured through conventional processes, there is a noted gap concerning the machining of polymeric parts that are created via additive manufacturing. This issue is critical as the properties of thermoplastic polymers, combined with the high temperatures required for machining, necessitate the optimisation of these processes to enhance the final performance of the components. The aim of this study is to provide a clear understanding of how to improve the machining of FFF PLA parts, which could be beneficial to meet the quality and efficiency standards required in modern industry.

The results support the identification of an application-oriented processing window for rotational PLA components

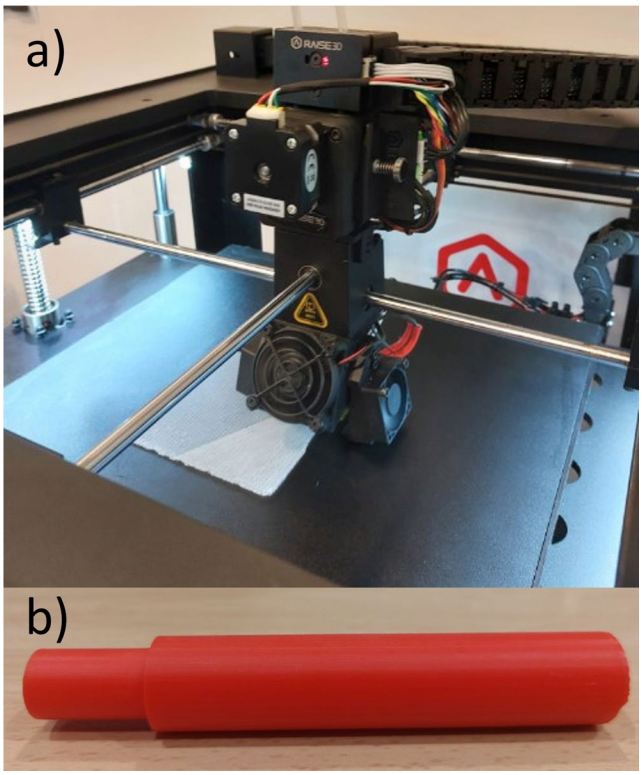

Fig. 1 **a** Model of the printer used in the experimental design; **b** Dimensions of the geometry to be obtained by FFF additive manufacturing in mm; **c** Final result

produced by FFF. This evidence is relevant to hybrid manufacturing workflows in which productivity targets must be balanced against requirements for surface integrity and process stability.

2 Materials and methods

The working material used as filament was PLA from Raise3D with a diameter of 1.75 mm. The geometry obtained using FFF technology is cylindrical, with a small recess in the diameter to fix the material on the claw plate. The FFF printing equipment used in this study was of the Raise3D brand, model Pro2 (Fig. 1.a). The nominal diameter of the cylinder is 20 mm and the length is 95 mm. Thus, the experimental study was divided into two manufacturing conditions based on the same cylindrical geometry. The first condition corresponds to specimens printed at a productive layer height and subsequently machined in turning to analyse the influence of cutting parameters. The second condition corresponds to the same cylindrical geometry printed using high quality parameters with a reduced layer height, used as a reference for comparison with the machined surfaces. A set of 12 specimens were printed by FFF and then

Table 1 Corresponding print parameters prior to machining tests

Layer height (mm)	0.3
Print speed (mm/s)	80
Filling density (%)	100
Filling pattern	Grid
Hot bed temperature (°C)	60
Extruder temperature (°C)	215

Table 2 High quality print parameters for further comparative analysis

Layer height (mm)	0.05
Print speed (mm/s)	60
Filling density (%)	100
Filling pattern	Grid
Hot bed temperature (°C)	60
Extruder temperature (°C)	215

machined to analyse the influence of cutting parameters on their surface quality (Fig. 1.b).

The printing parameters for this first stage are shown in Table 1 and the file has been laminated using the ideaMaker software. The printing time required for a cylindrical specimen with these parameters was 4 h and 30 min.

In parallel, to obtain the best possible quality using FFF technology and to be able to establish a comparison with the machining process, the same cylindrical geometry was produced with the following printing parameters (Table 2):

After obtaining the cylindrical geometries, an experimental design was carried out by means of a turning operation. The CNC equipment used was an EMCOTURN E45 turning centre. The cutting tool used was an uncoated WC insert, with ISO code DCMT 11T30814 IC20. The tool geometry is shown in Fig. 2.

It should be noted that, previously, a comparison was made with extreme combinations of cutting parameters (50 m/min, 0.05 mm/rev and 200 m/min, 0.2 mm/rev) to establish the influence of applying external air as a cooling agent. Subsequently, three levels of cutting speed (Vc) and four levels of feed rate (f) have been applied to establish the influence of both machining parameters on the final quality of the process. These combinations are shown in Table 3 and all the machining tests were carried out under the influence of external pressurised air to cool the process. The experimental campaign was designed as a full factorial 3×4 design, combining three levels of cutting speed and four levels of feed rate, resulting in twelve machining conditions.

The cutting speed and feed rate ranges were selected to represent practical turning conditions for thermoplastic materials while avoiding excessive thermal loading and unstable chip adhesion regimes in PLA. The selected levels were defined based on a combination of cutting tool manufacturer recommendations for machining polymer based materials and prior literature on thermoplastic machining

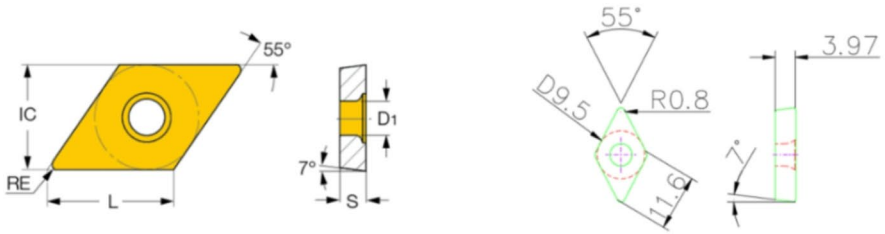

L (mm)	*IC* (mm)	*Vc* (mm)	*RE* (mm)	D_1 (mm)
11.6	9.52	3.97	0.80	4.40

Fig. 2 Main dimensions of the cutting geometry used in the experimental design

Table 3 Assembly of the pressurised air system on the CNC lathe and experimental design carried out

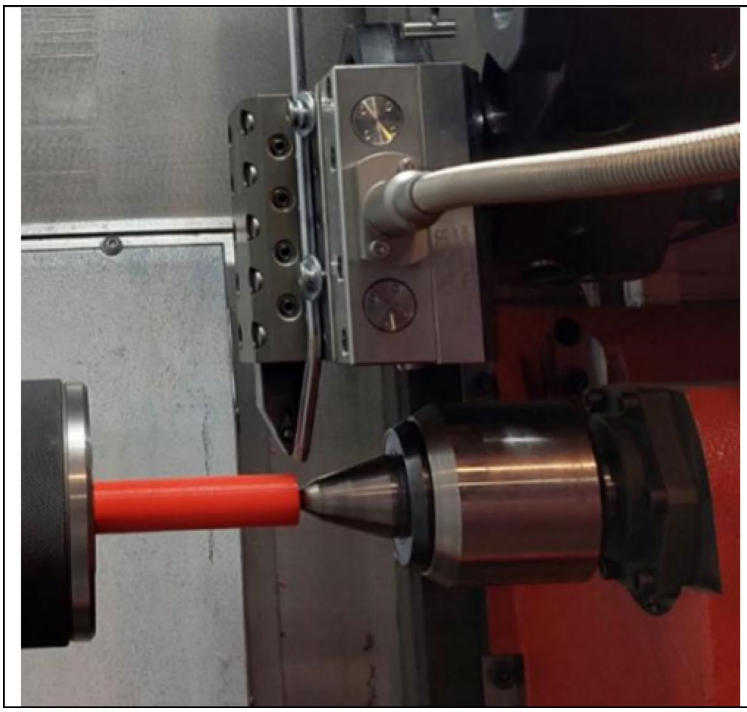

Vc (m/min)	*f* (mm/rev)	Cooling
50	0.05	No
200	0.20	No
50	0.05	Air
50	0.10	Air
50	0.15	Air
50	0.20	Air
125	0.05	Air
125	0.10	Air
125	0.15	Air
125	0.20	Air
200	0.05	Air
200	0.10	Air
200	0.15	Air
200	0.20	Air

behaviour. In particular, previous studies have shown that feed rate strongly governs material removal mechanics and temperature exposure time, whereas cutting speed mainly affects thermal softening through viscous deformation mechanisms in polymers [23]. These considerations guided the selection of cutting parameters to ensure process stability while enabling the analysis of thermomechanical effects relevant to post processing of material extrusion fabricated parts.

Parameter range definition and analysis approaches were informed by established machining optimisation and assisted cooling frameworks reported in recent manufacturing studies, including RSM-based multi-objective optimisation and advanced cooling strategies, which have been applied across different materials and processes [36, 37].

The depth of cut (a_p) was constant for all tests (1 mm). The machining operation consisted of a straight turning operation with a machining length of 60 mm.

During the machining process on the CNC turning centre, the maximum temperature generated in each test was monitored using a FLIR A6750 MWIR thermal imaging camera, located at 1.4 m from the machining centre (Fig. 3). In parallel, the cutting forces generated were monitored using a Kistler piezoelectric dynamometer that measure the three components of the cutting force located in the tool holder (*Fx*, *Fy*, and *Fz*). Finally, a Fluke Corporation 1732 Energy Logger network analyser was used to record the active energy consumption and active power for each machining test.

Each machining condition was performed once due to the experimental complexity and the extensive instrumentation

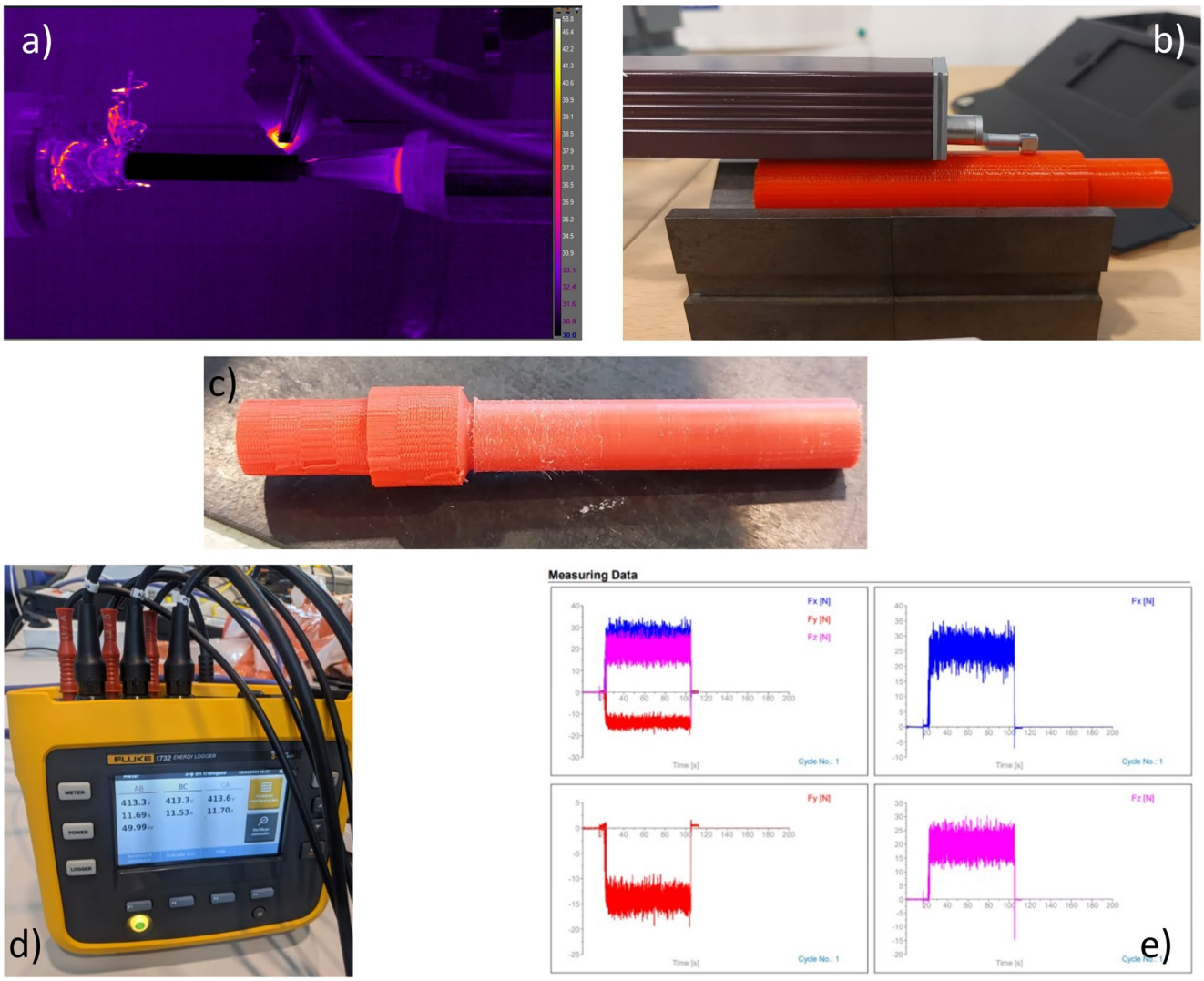

Fig. 3 Evaluation methodology: **a** Evaluation of temperatures using a thermographic camera; **b** Evaluation of surface quality using a roughness meter; **c** Machined part; **d** Network analyser to evaluate energy consumption; **e** Example of monitoring force signals during machining operations

required for simultaneous acquisition of temperature, force, and power signals. During each machining pass, temperature, cutting forces, and energy consumption were continuously recorded, providing time-resolved data representative of the specific cutting condition.

After the machining tests, a portable Mitutoyo roughness tester, model Surftest SJ-210, was used to evaluate the surface quality in terms of *Ra*, *Rz* and *Rt*. This evaluation was carried out both on the geometries after FFF manufacturing and after each machining test to establish a comparison. To account for variability in surface quality, eight surface roughness measurements were carried out on different generatrixes of each specimen in accordance with UNE EN ISO 4288, and the reported roughness values correspond to the average of these measurements. Consequently, variability is explicitly quantified for surface roughness, whereas force, temperature, and energy results represent condition-specific responses.

Each machining condition in the full factorial design was tested once, yielding a single set of output data per cutting condition. This strategy enabled coverage of the full parameter space while limiting material consumption and experimental time. Accordingly, the analysis is aimed at identifying trends and supporting mechanistic interpretation rather than quantifying pointwise repeatability.

The two printing conditions considered in the study were not experimental repetitions. All turning trials, including temperature, cutting force, and energy measurements, were performed only on specimens printed at a productive layer height of 0.3 mm and manufactured with machining allowances. Specimens printed at a reduced layer height of 0.05 mm were not machined and were used solely as a reference for surface quality comparison.

Surface temperature was measured using a radiometric FLIR A6750 infrared camera, factory calibrated against blackbody references using traceable standards. Emissivity was set to 0.95 for red PLA and the reflected apparent temperature to 23 °C. Based on a GUM-style uncertainty budget at a representative mean temperature of 100 °C, using normal propagation with a repeatability of 0.3 °C and conservative input uncertainties for emissivity and reflected radiation, the expanded uncertainty of temperature was estimated as ±2.5 °C (k=2), dominated by emissivity. Cutting forces were measured with a Kistler 9129AA dynamometer and a Kistler 5167A81 charge amplifier; manufacturer calibration certificates report axis-dependent CMC values of 0.11–0.28% (k=2) for the dynamometer, while amplifier deviations are below ±0.003%FSO.

3 Results

A key aspect for the correct machining of thermoplastic materials is the influence of an external coolant such as the application of pressurised air. The first results were carried out without the application of air. In these tests, in different machining conditions, a poor surface finish was observed, with a very rough surface and in worse condition than the initial condition one (Fig. 4). This is due to the low melting temperature of the thermoplastic material in PLA. The machined chip, when evacuated, re-adheres to the surface of the material due to the low melting temperature of the thermoplastic material. The generated chip reaches temperatures close to, or even equal to, the melting point of the material and, upon contacting the surface, re-welds to it, making its later removal difficult [23, 38].

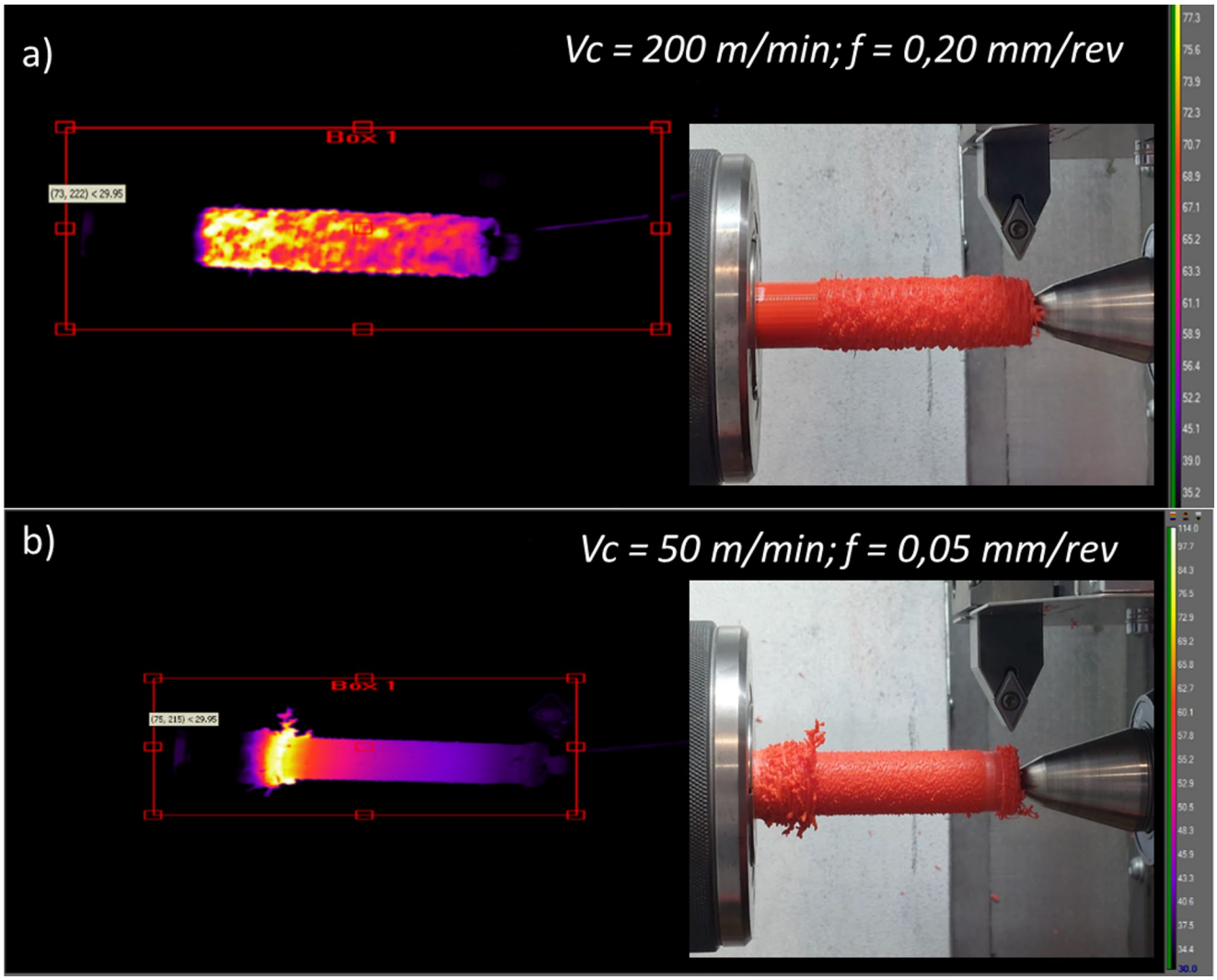

Fig. 4 Influence of cutting parameters without the application of air as a coolant on the maximum temperatures developed during the machining process

This can be observed from the thermal field measured using the infrared camera and represented as thermograms in Fig. 4. The recorded temperature distribution reveals a marked thermal gradient across the freshly machined surface, consistent with localised heat accumulation promoted by chip re-adhesion and smearing on the polymer surface.

The results reveal a significant influence of cutting parameters on surface quality. While both cases show a poor surface finish, a low combination of cutting speed and feed rate results in a higher accumulation of chips adhering to the tool during the process. This substantially increases the maximum process temperature and generates a larger chip nest at the end.

Subsequently, these same tests were carried out by applying a pressurised air system directed towards the cutting tool. The aim is both to combine increased cooling during the machining process and to favour the evacuation of the chip, avoiding its re-adherence to the surface (Fig. 5) [39]. The cooling effect in the machining process can be observed in Fig. 5. For low *Vc* and *f* (50 m/min, 0.05 mm/rev), the pressurised air application reduces the temperature up to 40 °C (about a 30%) eing a significant influence in the reduction of the chip adhesion. Nevertheless, the pressurised air effect in the temperature for higher *Vc* and f (200 m/min, 0.20 mm/rev) is less significant, reducing the temperature about 10 °C. Therefore, under these conditions of cutting parameters, the pressure over the chip it is more relevant.

Having established the need for a pressurised air-cooling system, the influence of different combinations of cutting parameters on the maximum process temperature has been evaluated. The correct selection of cutting parameters is essential in the machining process. Very high maximum temperatures are a critical parameter in the machining of thermoplastic materials, which can affect their mechanical performance and affect other variables such as surface integrity or geometric deviation.

Figure 6 illustrates the evolution of the maximum temperature during the turning of FFF-fabricated PLA under the analysed cutting conditions. An increase in cutting speed led to a clear rise in thermal loading, whereas higher feed rates limited temperature accumulation due to reduced tool–material contact time. These results highlight the thermally driven nature of PLA machining, while confirming that compressed-air assistance effectively mitigates excessive heat build-up during the machining pass.

Considering the mean behaviour, both cutting speed and feed rate affected the thermal response. Cutting speed primarily increased thermal loading, whereas higher feed rates reduced heat accumulation by shortening the tool material interaction time. This indicates that, under the selected conditions, feed rate acts mainly as a time exposure control parameter while cutting speed governs the intensity of thermomechanical heating.

Thus, increasing the feed rate to 0.20 mm/rev reduces the exposure time of the material to interaction with the cutting tool, reduces operating times and minimises the maximum temperatures reached. Similar results occur in the drilling of PEEK thermoplastic material. In the study by Chang et

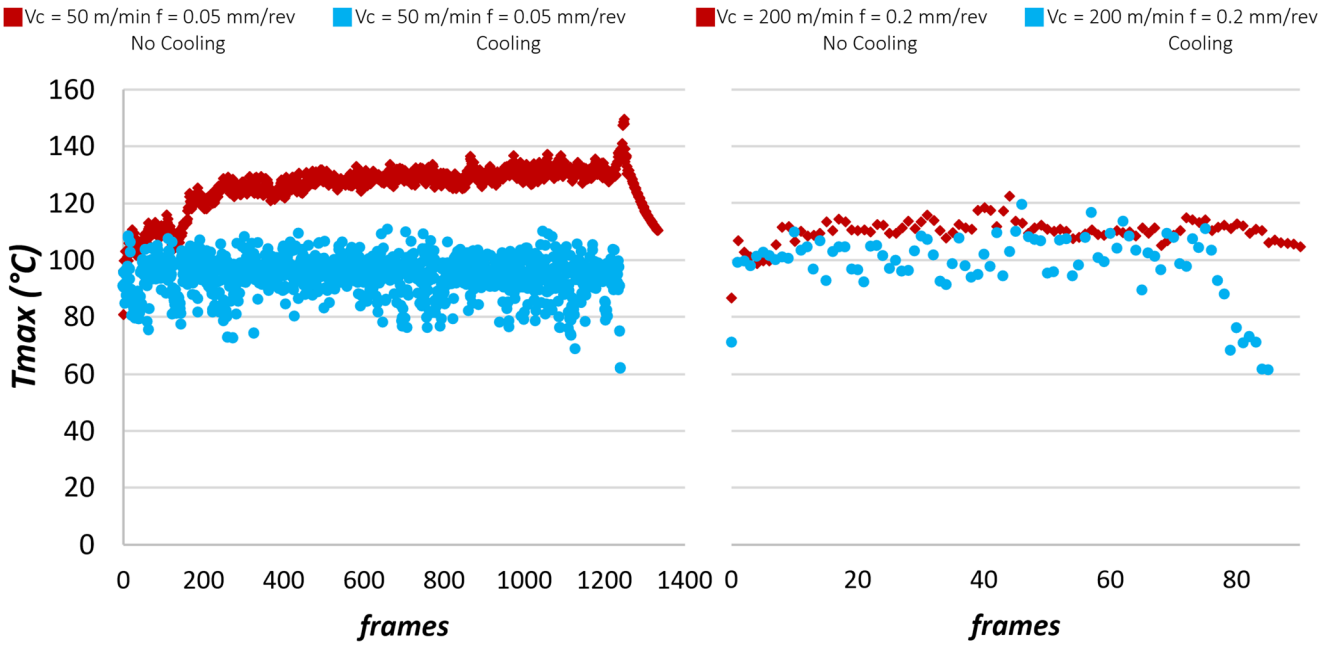

Fig. 5 Influence of pressurised air as a coolant on the maximum temperature recorded during a turning operation for extreme cutting parameter combinations. **a** Comparison with air (WA) and without air (NA) for a cutting speed of 50 m/min and a feed rate of 0.05 mm/rev; **b** Comparison with air (WA) and without air (NA) for a cutting speed of 200 m/min and a feed rate of 0.2 mm/rev

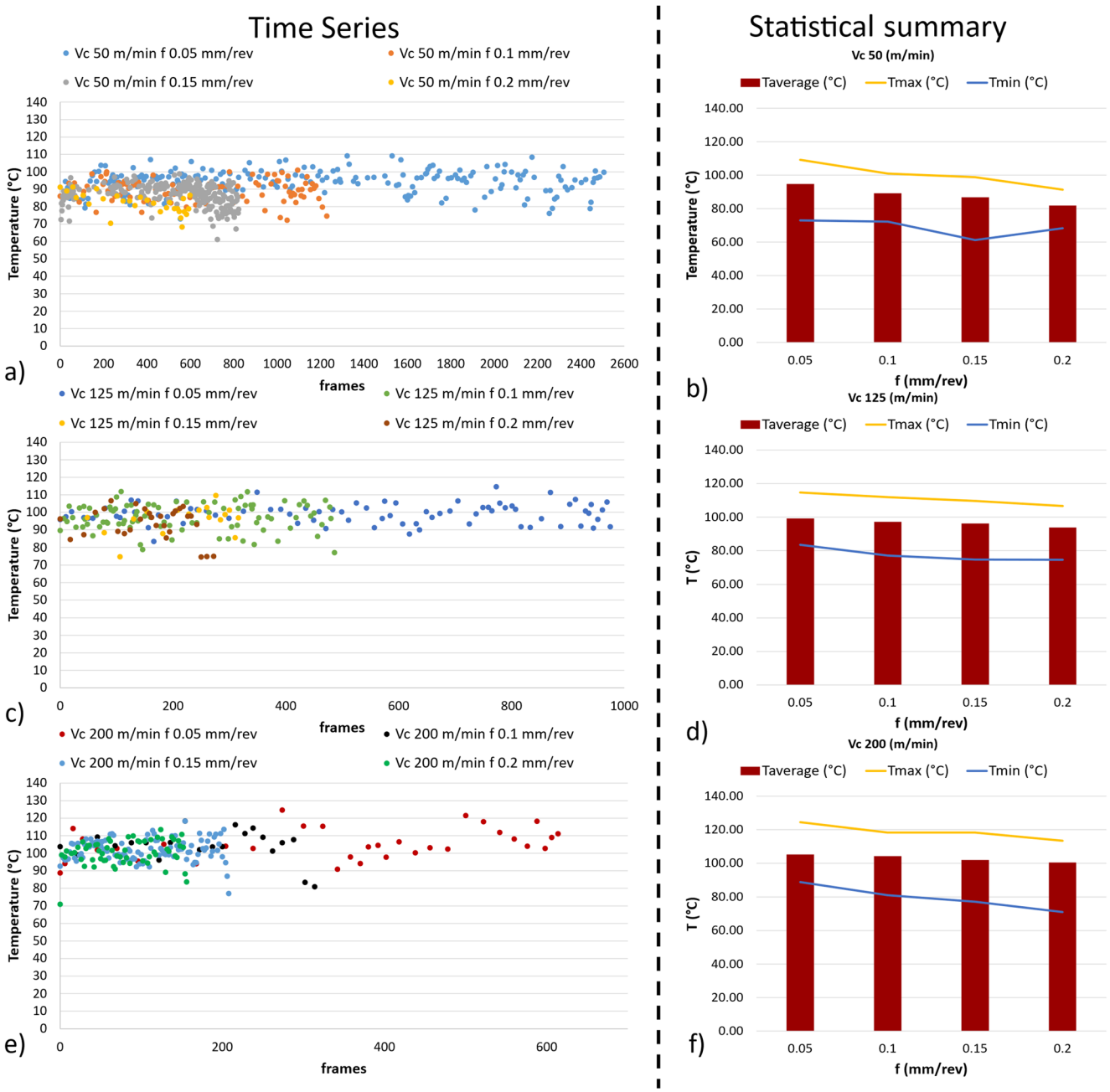

Fig. 6 Representation of the record of maximum temperatures obtained in each turning operation for: **a** Vc 50 m/min; **c** Vc 125 m/min; **e** Vc 200 m/min. Representation of the maximum, minimum and average value within the range of maximum temperatures reached for: **b** Vc 50 m/min; **d** S 125 m/min; **f** Vc 200 m/min. Panels (**a**), (**c**) and (**e**) show time-series of Tmax versus time. Panels (**b**), (**d**) and (**f**) report the corresponding statistical summary of Tmax for each condition, including minimum, maximum and mean values

al. [40] have been observed that the temperature within the machining area is inversely proportional to the feed rate. This means that a higher feed rate can help to form regular curly chips, which is beneficial for controlling the temperature during machining.

However, by increasing the cutting speed from 50 m/min to 125 m/min and 200 m/min, the effect of the feed rate is reduced. An increase in this parameter implies a higher friction between the main cutting edge of the tool and the surface of the material, generating a larger volume of machined material. However, this increase results in greater plastic deformation of the thermoplastic material, leading to an increase in the heat generated by the chip. Most of the energy used in the plastic deformation during cutting is converted into heat, raising the temperature in the cutting zone. The results showed that viscous deformation caused

by temperatures above the glass transition temperature (*Tg*) of the polymers played a decisive role in the surface quality of these materials. Li et al. [41] showed that the glass transition temperature decreases significantly with pressure and temperature, which directly affects the machinability of the material. Based on the experimental results, it was found that the best conditions for surface quality were high feed rates and low cutting speeds.

At the highest cutting speed, the process operated closer to a thermally critical regime, with greater sensitivity to heat accumulation. This reinforces that temperature related outcomes should be interpreted as predominantly controlled by cutting speed, while feed rate moderates exposure time and thereby limits the severity of thermal peaks. This can negatively affect the final quality of the machined part. An example occurs in the machining of polymer matrix composites. In the case of fibre-reinforced thermoplastic composites, such as reinforced carbon tubes, the heat generated by the machining process can affect the polymer matrix, altering the surface characteristics and properties of the material [42].

The observed temperature response indicates that the turning of FFF fabricated PLA is governed by thermally driven material behaviour. As the cutting zone temperature increases, PLA approaches a viscoelastic regime where the apparent flow stress decreases and the material exhibit greater ductility. This thermal softening reduces the resistance to shearing and promotes smoother chip separation, which is consistent with the reduced sensitivity of force components to cutting speed within the analysed range. Feed rate primarily controls the duration of tool material interaction, so higher feed rates reduce exposure time and limit heat accumulation, thereby moderating the extent of softening. The combination of low thermal conductivity and the layered architecture inherent to FFF can locally intensify heat accumulation and promote intermittent chip adhesion on the rake face, which may contribute to force variability and to the surface integrity outcomes observed under the most thermally demanding conditions.

In turn, these temperature variations may be due to factors such as friction, time contact between tool cutting edge and material, the heating of the cutting tool or the low thermal conductivity of PLA, which has difficulty in dissipating heat. Furthermore, although the chip generated is constantly blown away by the compressed air, the images captured by the thermal imaging camera show that the chip continues to stick at the surface of the material and some of it is dragged away by the cutting tool until the end of the machining process (Fig. 7).

Beyond chip evacuation behaviour, the condition of the cutting tool was examined to evaluate its potential contribution to the observed trends. After completion of the machining trials, the insert was inspected for wear or damage that could have affected the measured responses. No relevant wear features were detected under the selected cutting conditions, and no measurable degradation of the cutting edge was identified. Accordingly, tool wear was not considered

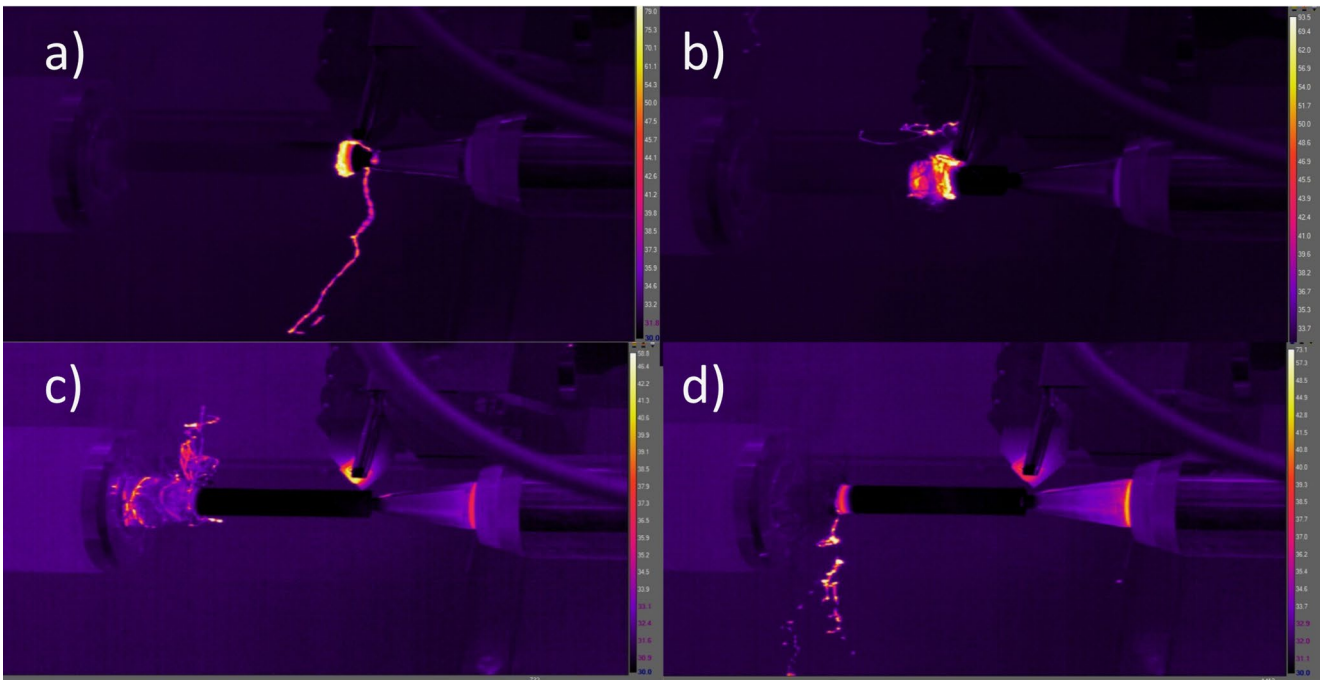

Fig. 7 Evolution of the chips generated and temperature dissipation during the machining process for: **a** a combination of Vc 125 m/min and f 0.15 mm/rev at initial machining; **b** Half machining; **c** End of process; **d** End of process at combination of Vc 125 m/min and f 0.05 mm/rev

a dominant factor within the scope of this study and was therefore not included as a dedicated analysis.

When turning thermoplastics, some of the heat generated is dissipated through the chips. At higher feed rates, the chips are thicker and can carry more heat away from the cutting zone. This can help reduce the temperature at the tool-material interface, benefiting the process by reducing the risk of thermal deformation of the material and thermal degradation of the tool.

At the beginning of the process, it can be seen how the continuous chip is being properly evacuated (Fig. 7.a). However, it starts to adhere to and wrap around the workpiece (Fig. 7.b). Finally, it is dragged by the cutting tool to the end of the operation, where it accumulates near the jaw chuck (Fig. 7.c). In operations where the feed rate is lower, more time is available for chip removal (Fig. 7.d). However, it has been found that at the end of the process there is still chip accumulation, but to a lesser extent.

From a mechanistic standpoint, the force response should be interpreted together with the thermomechanical state of PLA, where cutting speed influences thermal softening while feed rate governs mechanical engagement and chip formation stability.

Figure 8 summarises the cutting force components for the analysed turning conditions. The dominant trend is governed by feed rate, which increases mechanical engagement and therefore raises the force levels. Cutting speed showed a limited direct influence on force magnitude within the studied range, although it modifies the thermomechanical state of the cut through its effect on temperature.

On the other hand, the cutting speed does not seem to have a significant impact, since, for different cutting speeds, the values of the force are numerically very close to each other.

Although cutting speed did not exert a statistically significant effect on the cutting force components within the

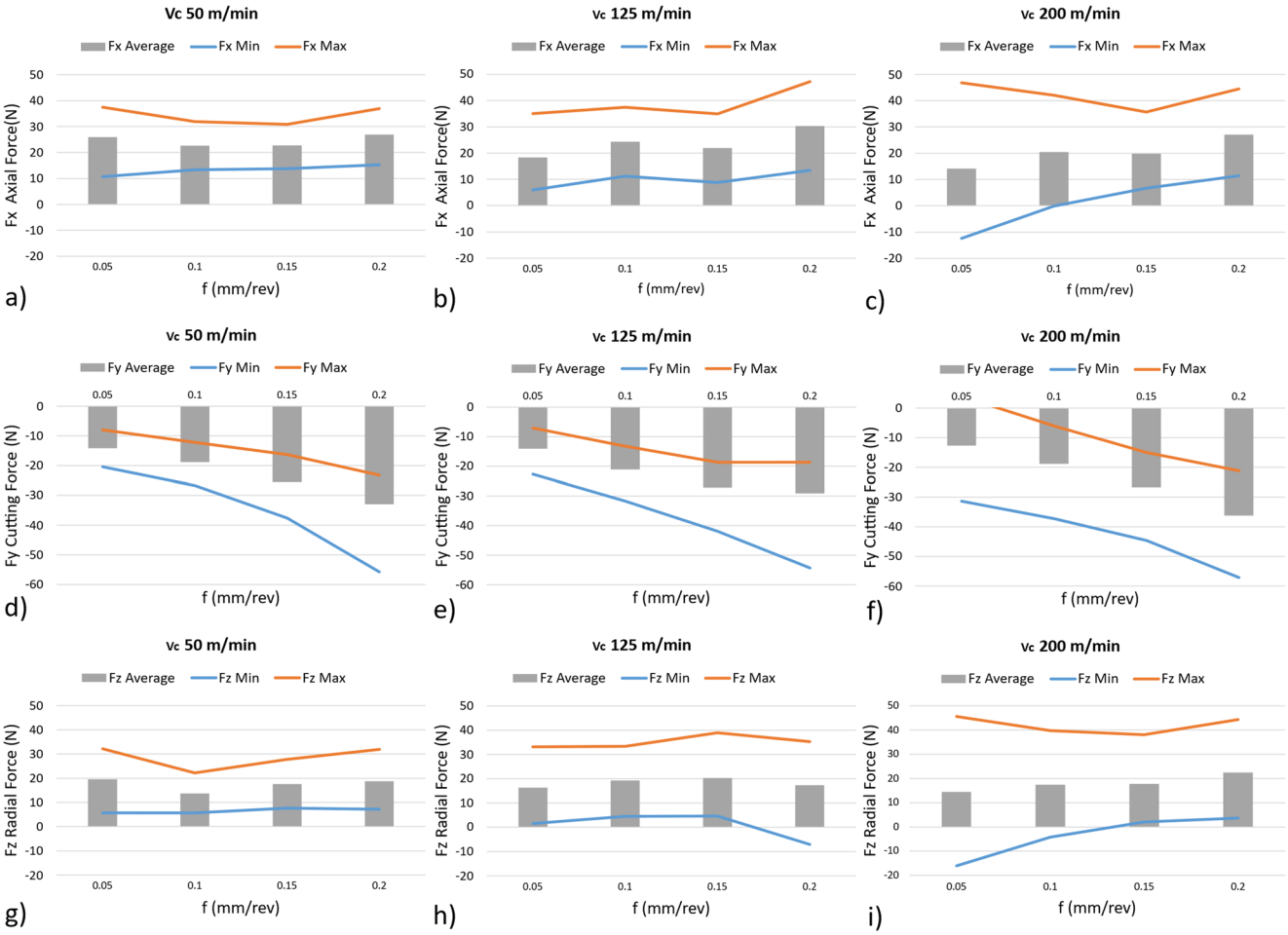

Fig. 8 Cutting force components measured during turning of FFF-fabricated PLA under compressed-air conditions. **a** Axial force Fx at cutting speed Vc = 50 m/min. **b** Axial force Fx at Vc = 125 m/min. **c** Axial force Fx at Vc = 200 m/min. **d** Cutting force Fy at Vc = 50 m/min. **e** Cutting force Fy at Vc = 125 m/min. **f** Cutting force Fy at Vc = 200 m/min. **g** Radial force Fz at Vc = 50 m/min. **h** Radial force Fz at Vc = 125 m/min. **i** Radial force Fz at Vc = 200 m/min. For each feed rate, grey bars denote the mean force, while the blue and orange lines indicate the minimum and maximum values, respectively. All forces are reported in newtons, and the x-axis corresponds to feed rate

investigated range, its indirect influence on the machining response should be acknowledged. Higher cutting speeds increased the cutting zone temperature and produced measurable changes in energy consumption. These thermal effects are likely to promote local softening of the PLA matrix, which may partially offset mechanical resistance during chip formation. Consequently, cutting speed primarily modifies the thermomechanical conditions of the operation rather than directly governing the cutting forces, for which feed rate remained the dominant controlling factor.

The strength is highly dependent on the material of the workpiece. PLA is a material that offers little resistance to machining due to its mechanical properties. This fact, coupled with the cutting depth of cut is only 1 mm, the cutting edge of the tool is sharp, without any tool wear and the geometry of the cutting tool is designed for machining soft materials, has resulted in very small cutting force values.

The axial force (Fx) related to the depth of cut of the tool in the material generally shows values between 20 N and 30 N. However, for cutting speeds of 125 m/min and 200 m/min, this force seems to show an upward trend. As the feed speed increases, although the depth remains constant, the volume of material removed increases, which requires a higher force to machine the material correctly. However, it is remarkable the wide range observed between the minimum and maximum force generated in this axis when Vc is 200 m/min and f is 0.05 mm/rev. This combination coincides with the maximum temperature peak and a possible higher accumulation of chips adhering to the cutting edge during the turning process. This may affect the variability of the force generated associated with the adhesion and detachment of the thermoplastic material chip itself. As the feed rate increases, the tooth of the tool must remove a greater amount of material per unit of time. This requires greater force to penetrate and cut the material, which results in an increase in radial cutting force. Thermoplastic materials, due to their nature, can offer variable cutting resistance, depending on their mechanical properties at different temperatures. At higher feed rates, the material is less able to plastically deform and offer shear strength, resulting in an increase in the radial force required for material removal [43].

In the machining of thermoplastics, heat generation is a critical factor due to the low thermal conductivity of these materials. A shorter contact time reduces the amount of heat generated in the cutting zone and, therefore, may lead to a reduction in cutting temperature. Furthermore, at higher feed rates, the generated heat has less time to transfer from the cutting zone to the tool and the material itself, which can contribute to lower heat accumulation in the piece and the tool.

For the radial component, forces increased with feed rate because of higher instantaneous material removal. No cutting condition produced forces high enough to trigger interlayer separation or macroscopic damage of the printed structure, indicating stable machining of the selected build configuration.

Similarly to the axial force, the radial cutting force increases with increasing feed rate. As the feed rate increases, the interaction time between the thermoplastic material and the cutting edge is drastically reduced. This minimises the friction between the tool and the material and decreases the cutting temperature. This is key due to the thermoplastic nature of PLA. By increasing the feed rate parameter, the risk of reaching the glass transition point is reduced, which in turn results in an increase in the cutting force because the material exhibits a more rigid state.

The thrust component followed a similar pattern, with feed rate governing the magnitude and cutting speed affecting variability only secondarily. This behaviour supports the interpretation that mechanical loading is primarily controlled by feed related engagement, while thermal effects associated with cutting speed play a secondary role in the force response.

The resultant of the forces generated during each turning test is shown in Fig. 9. At the lowest feed rate, higher cutting speed reduced the resultant force, which is consistent with thermally assisted softening of the polymer in the cutting zone. As feed rate increased, mechanical engagement dominated and the influence of cutting speed on the resultant force became less pronounced. As the cutting speed increases, the material tends to heat up in the contact zone with the tool. Thermoplastics, being sensitive to temperature, can soften when exposed to high temperatures, which reduces their cutting resistance. This means that less force is required to remove the material, resulting in a decrease in the resultant force [44, 45]. Furthermore, with higher cutting speeds, the increase in temperature in the cutting zone can lead the material to undergo plastic deformation more easily rather than elastic deformation, which requires less mechanical effort from the cutting tool to remove the material. Additionally, increasing the cutting speed reduces the contact time between the tool and the material per revolution, decreasing the effective contact area and therefore the necessary cutting force. This effect is particularly notable in materials such as thermoplastics, where thermal conductivity is low and generated heat can quickly concentrate, affecting the mechanical properties of the material in the cutting zone.

On the other hand, as the feed rate increases, the effect of cutting speed is minimized or nullified, with increasing values in the resultant force for all levels of cutting speed (Vc). At higher feed rates, more material is removed per unit

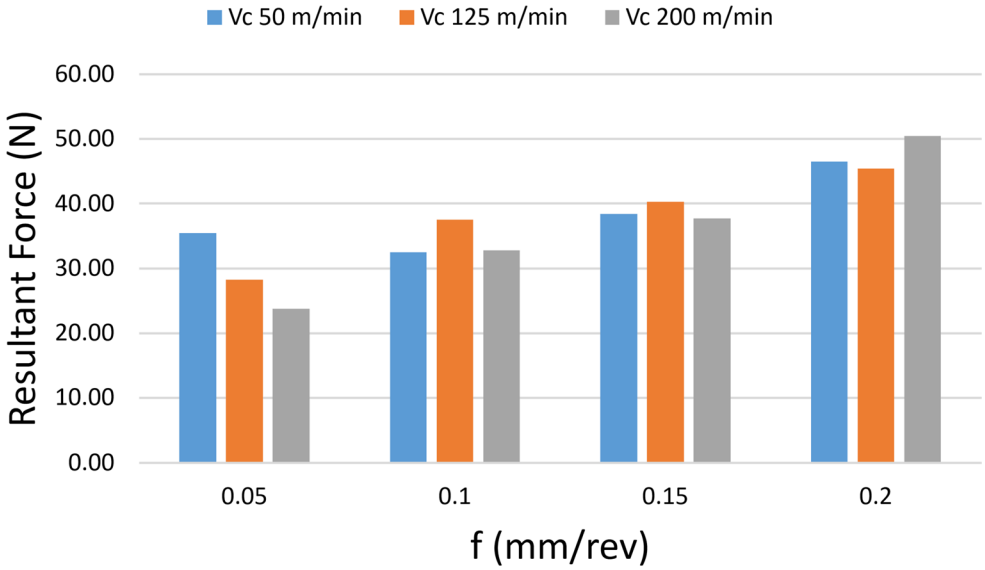

Fig. 9 Resultant cutting force during turning of FFF-fabricated PLA under compressed-air conditions as a function of feed rate and cutting speed. The resultant force represents the overall machining load obtained by combining the three measured force components into a single magnitude, accounting for the axial, cutting and radial contributions

of time, requiring an increase in cutting force regardless of cutting speed. At high feed rates, the proportional contribution of material resistance to the resultant force increases, making variations in cutting speed have a lesser impact on reducing the resultant force. Although higher cutting speeds generate more heat, at higher feed rates, the duration of contact between the tool and any specific point on the material is shorter. This limits the amount of heat absorbed by the material and the tool, reducing the softening effect of the material that could decrease the resultant force at high cutting speeds. Therefore, the effect of heat on reducing the resultant force is attenuated.

Furthermore, at high feed rates, the plastic deformation necessary to remove the material becomes the dominant factor determining the resultant force, rather than the thermal effects caused by high cutting speeds. The force required to deform and cut the material becomes the primary contribution to the resultant force, reducing the relative influence of cutting speed.

Figure 10 summarises the energetic response of the turning tests in terms of active power and accumulated energy. Active power increased with cutting speed, consistent with higher spindle demand. In contrast, accumulated energy was primarily driven by machining time, so higher feed rates reduced total energy demand by shortening the cutting pass. Overall, productivity related parameters governed energy efficiency, while cutting speed influenced the instantaneous power level and the associated thermal response.

These results do not allow us to conclude that the other output variables analysed in the machining operation, such as T and Fy, influence the P required for material removal, since it cannot be established that the machining operation itself has a significant effect on the mechanical characteristics of the material machined, as could be the case with metallic materials.

In terms of active energy consumed during cutting (Fig. 10b), an increase in Vc tends to reduce the value of E. However, the effect of f on E is more significant than the effect of Vc. In this case, an increase in f also tends to reduce the value of E to a greater extent, its influence being much more noticeable at low values of Vc (50 m/min). This behaviour is mainly due to the time required to perform the cutting operation, where increases in Vc and f tend to reduce their value. The cutting time and the active power are directly related to the value of the energy consumed, and since the reduction of the cutting time is much more relevant than the increase of the active power, the value of E tends to decrease.

Finally, to continuous in the study of the machinability of PLA in parts obtained by additive manufacturing (FFF), a study of the surface quality obtained under different conditions has been conducted (Fig. 11).

On one hand, the influence of cutting parameters in a turning operation on the roughness obtained in terms of Ra, Rq, and Rz has been studied. Additionally, the same geometry has been obtained exclusively through additive manufacturing, modifying the layer height parameter (0.05 mm, 0.3 mm), and the obtained surface quality has been evaluated.

The comparison confirms that turning substantially improves surface finish relative to as printed specimens, independent of the selected layer height. Fine layer printing improves surface quality at the expense of build time, whereas the hybrid route based on productive printing followed by turning achieves comparable or superior surface finish with markedly improved throughput. In combination, by establishing high-quality printing parameters with a layer

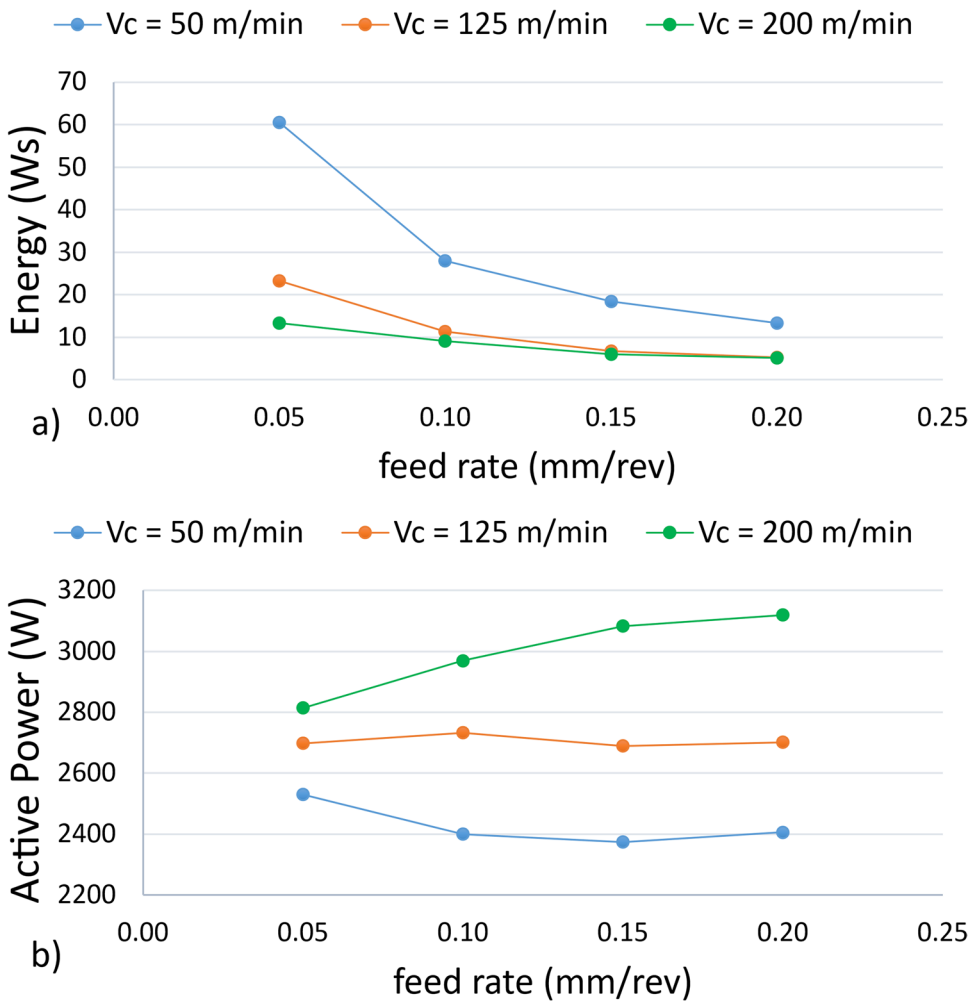

Fig. 10 Influence of cutting parameters in each turning operation on: **a** Consumed energy; **b** Active power

height of 0.05 mm, a surface quality in terms of *Ra* of 6.28 µm has been obtained, resulting in very different surfaces as observed in Fig. 12 [46].

Feed rate was the dominant factor controlling the roughness metrics, with higher values generally improving surface finish under compressed air assistance. The combined effect of reduced thermal exposure and more stable chip evacuation contributed to a more homogeneous machined surface, consistent with the observed links between temperature, cutting behaviour and surface integrity. These values are of interest and close to the established limit for surface quality in machining of composite materials in the aerospace sector. This confirms the influence of these cutting parameters and the relationship between surface quality, cutting temperatures, and forces generated during the process. Specifically, the application of an air-cooling system that facilitates the evacuation of thermoplastic chips, combined with a correct selection of machining cutting parameters, allows for a more homogeneous surface free of re-adhered material on the machined surface.

On the other hand, an increase in feed rate leads to a reduction in temperatures as seen previously. The nature of the thermoplastic material, combined with less exposure to interaction with the cutting tool, allows for a more stable machining process without the risk of reaching temperature peaks close to the glass transition temperature. This results in better chip evacuation and a more efficient process, achieving a surface with reduced roughness and homogeneous characteristics, as a similar trend is observed in *Ra*, *Rz*, and *Rq*.

The fact that increasing the feed rate improves surface quality establishes an improvement in terms of production by requiring less machining time and active energy consumption to achieve an optimal result, thereby enhancing process performance.

From a productivity perspective, the hybrid approach shifts surface finish requirements from the printing stage to a controlled finishing operation. This reduces total production time for rotational parts when compared with fine layer printing, especially in batch scenarios where machining setup times are amortised across multiple components.

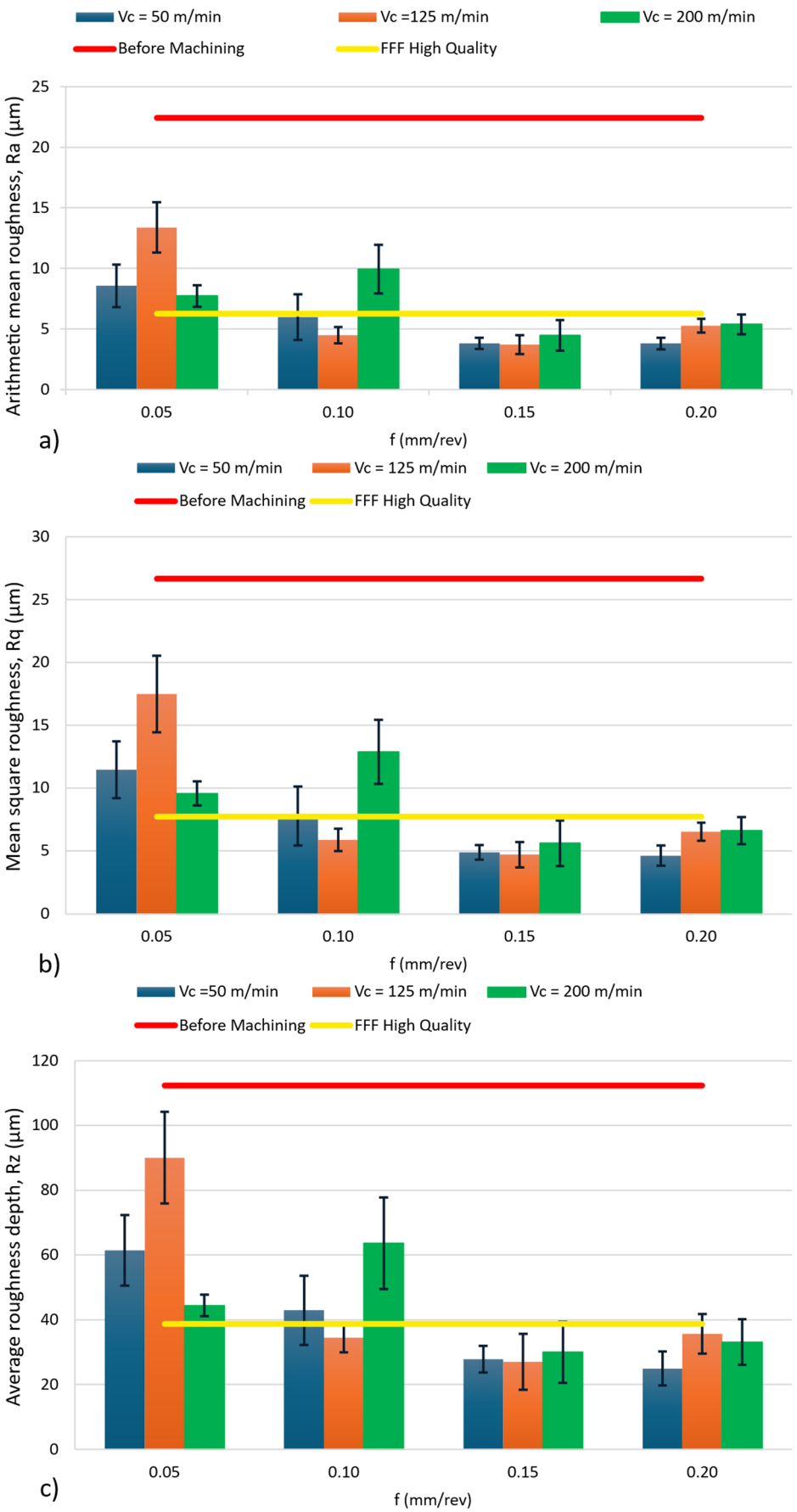

Fig. 11 Influence of cutting parameters in each turning operation on the surface quality evaluated in terms of: **a** Ra; **b** Rq; **c** Rz

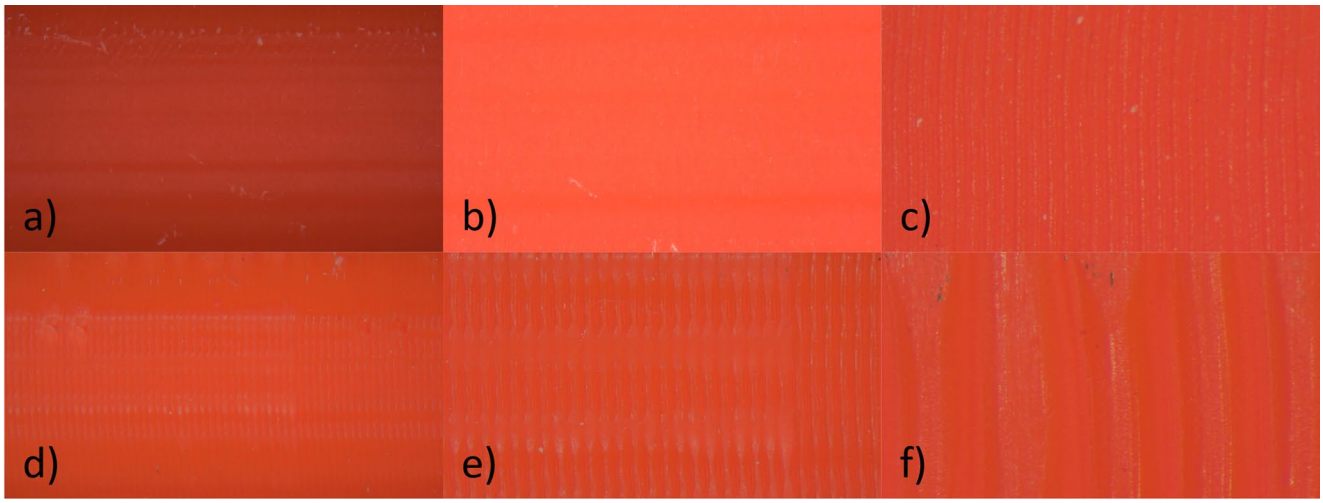

Fig. 12 Macrographs of the surface quality of a geometry printed with a layer height of 0.05 mm (Ra = 6.28 μm) at: **a** 8X; **b** 16X; **c** 100X and of a geometry printed with a layer height of 0.3 mm (Ra = 22.41 μm) at: **d** 8X; **e** 16X; **f** 100X

This indicates the effectiveness and interest of establishing turning as a secondary operation combined with additive manufacturing to achieve high quality rotational parts. Although very low roughness values are achieved when using a layer height of 0.05 mm, the turning stage still provides a robust route to generate a cutting produced surface whose final quality can be further improved by selecting appropriate cutting parameters, particularly feed rate, under compressed air assistance. From a productivity perspective, the high-quality printed geometry with a layer height of 0.05 mm required 14 h of printing time. In comparison, the specimens manufactured for machining required 4 h of printing time at a productive layer height, followed by a short finishing operation, with a maximum turning time of 86 s. However, in addition to the net machining time, periods associated with CNC start up must be considered, including setup, fixturing, tooling preparation and tool changeovers. These intervals precede the process and remain essentially constant, so their relative impact is reduced as batch size increases. Consequently, for batch production of FFF parts designed with machining allowances, the combined route becomes more productive than manufacturing parts exclusively by high quality FFF to final dimensions, since the overall time is optimised by transferring surface and dimensional requirements from a long printing stage to a controlled and repeatable finishing operation.

The productivity comparison presented in this work is based on a systematic evaluation of process time components. Printing time is treated as a variable dependent on layer height and build strategy, whereas CNC related setup operations including machine startup, fixturing, tool setting and tool change are assumed to be constant for a given batch. Under these assumptions, the relative impact of setup time decreases as batch size increases, while the reduction in printing time achieved by using a productive layer height becomes dominant. Consequently, the productivity advantage of the hybrid FFF plus turning approach is particularly relevant for batch production scenarios, whereas for single part manufacturing the difference between both strategies is reduced by fixed setup overheads.

Several post processing routes have been reported to enhance the surface quality of PLA components, including manual finishing operations such as sanding and polishing, chemical or solvent based smoothing, coating treatments, and CNC machining processes such as milling [47]. The suitability of these approaches depends on part geometry and functional requirements [48]. However, they commonly entail either high labour input, limited dimensional control, or constraints associated with surface accessibility and, in the case of solvent processes, safety and handling requirements.

By contrast, turning offers a controlled and repeatable finishing operation for axisymmetric parts. It enables removal of the characteristic extrusion induced surface texture while improving surface finish under well-defined cutting conditions [34]. The use of compressed air in this study further supported process stability by reducing chip adhesion and limiting thermal loading. Nevertheless, turning remains restricted to geometries compatible with lathe operations, and non-axisymmetric or highly featured parts may be better served by alternative post processing strategies. Turning should therefore be regarded as a complementary option within hybrid manufacturing routes for PLA components, particularly when rotational geometry, batch productivity, and process repeatability are prioritised [49].

Machining as a secondary operation is particularly advantageous when rotational or axisymmetric geometries are involved, where turning enables direct control of surface

finish and dimensional accuracy. This approach is especially beneficial in batch production scenarios, where CNC setup operations are amortised across multiple parts and printing time can be reduced by adopting a productive layer height. In contrast, fine layer FFF printing remains preferable for single part manufacturing, geometries with limited post processing accessibility, or components dominated by complex non rotational features. Therefore, the choice between high quality FFF printing and machining assisted finishing should be guided by geometry, batch size, and functional surface requirements rather than by surface roughness alone.

While the effects of cutting parameters on surface roughness and cutting temperature have been reported for thermoplastic machining, much of the literature focuses on conventionally processed polymers or on isolated post processing outcomes for additively manufactured parts. The present study addresses the machinability of Fused Filament Fabrication PLA through an integrated experimental framework, in which cutting temperature evolution, cutting forces, energy consumption, and surface roughness are analysed under the same turning conditions. This enables a consistent interpretation of the thermomechanical response of FFF manufactured PLA in a temperature regime where material behaviour becomes strongly temperature dependent as the glass transition is approached.

In parallel, several alternative post processing techniques have been shown to reduce surface roughness, including chemical vapour treatments for PLA and mechanical finishing routes such as ball burnishing. However, these approaches may involve limitations in dimensional control, part accessibility, or repeatability, depending on geometry and process conditions. Chemical vapour treatment of FFF PLA has been reported as an effective route for surface finish improvement [31]. Mechanical post processing by ball burnishing has also been proposed as a viable option for FFF parts, with reported improvements in surface quality and functional performance [32].

CNC based post processing of material extrusion parts has been explored primarily from the perspective of surface quality enhancement [34]. In contrast, the present work extends this perspective by correlating surface integrity improvement with process temperature, mechanical loading, and energy demand. The results therefore provide an application-oriented basis for assessing turning as a post processing route for FFF PLA, particularly for rotational geometries where controlled machinability, productivity, and process stability are critical.

In general terms, the influence of cutting parameters in a turning operation is presented in Table 4 through an ANOVA statistical analysis. Throughout this section, ANOVA outcomes are used to support statistical claims regarding factor effects. Only effects with p-values below 0.05 are described as statistically significant within the adopted framework. When p-values are marginal or above this threshold, the corresponding patterns observed in the experimental data are discussed as qualitative trends and are not presented as statistically confirmed effects. This tool is used to determine if there are significant differences between the means of three or more independent groups, considering multiple input variables or factors.

The ANOVA was performed using a regression-based approach where cutting speed and feed rate were treated as continuous predictors. A second order model including linear, quadratic, and interaction terms was considered, hence each term has one degree of freedom.

The analysis of variance (ANOVA) was applied to identify the relative influence of cutting parameters on the measured outputs. Prior to interpretation, the suitability of the data for ANOVA was assessed considering the underlying assumptions of normality, independence, and homoscedasticity. The independence of observations was ensured by the experimental design, as each machining condition corresponded to a distinct parameter combination. Given the limited number of repetitions per condition, normality and homoscedasticity were evaluated through inspection of residual distributions and variance trends rather than formal hypothesis testing. Within these constraints, the ANOVA results are interpreted as indicative of dominant parameter effects rather than as strict confirmatory statistical inference.

Effects associated with p-values below 0.05 are discussed as statistically significant within the adopted ANOVA framework. When p-values are marginal or above this threshold, the corresponding observations are described as trends or qualitative behaviours supported by the experimental data, and they are not presented as statistically confirmed effects.

Thus, it allows identifying which of the input variables have a statistically significant impact on the dependent variable. Within this analysis, a high F-value and a low p-value suggest that there is significant statistical evidence to assert that at least one of the group means is different from the others. As seen previously in the results, in all output variables except for the maximum recorded temperature, the feed rate parameter is statistically significant. Cutting speed did not show a statistically significant effect on Fx ($p = 0.063$); however, the mean values suggest a modest decreasing trend at the lowest feed rate, which may be associated with thermally driven softening.

Components produced by Fused Filament Fabrication inherently exhibit anisotropic mechanical behaviour due to layer wise deposition and direction dependent interlayer bonding. In this study, all specimens were manufactured using identical printing parameters and a fixed build orientation to minimise variability associated with the deposited

Table 4 ANOVA statistical analysis of the input variables on the different output variables evaluated

Source	GL	SC Ajust.	MC Ajust.	F-Value	*p*-Value
Ra					
Vc (m/min)	1	3.5431	3.5431	0.64	0.455
f (mm/rev)	1	48.7	48.7	8.76	0.025
Error	6	33.3412	5.5569		
Total	11	98.0935			
Rq					
Vc (m/min)	1	4.382	4.382	0.45	0.529
f (mm/rev)	1	90.052	90.052	9.15	0.023
Error	6	59.046	9.841		
Total	11	173.766			
Rz					
Vc (m/min)	1	24.51	24.51	0.10	0.762
f (mm/rev)	1	2189.89	2189.89	8.99	0.024
Error	6	1462.28	243.71		
Total	11	4186.93			
Taverage					
Vc (m/min)	1	442.077	442.077	395.64	0.000
f (mm/rev)	1	93.912	93.912	84.05	0.000
Error	6	6.704	1.117		
Total	11	560.188			
Tmax					
Vc (m/min)	1	693.409	693.409	174.40	0.000
f (mm/rev)	1	221.222	221.222	55.64	0.000
Error	6	23.856	3.976		
Total	11	955.752			
Pactive					
Vc (m/min)	1	648,159	648,159	252.87	0.000
f (mm/rev)	1	5939	5939	2.32	0.179
Error	6	15,379	2563		
Total	11	720,709			
Energy					
Vc (m/min)	1	939.9	939.86	45.18	0.001
f (mm/rev)	1	934.1	934.06	44.90	0.001
Error	6	124.8	20.8		
Total	11	2674.1			
Fx					
Vc (m/min)	1	35.701	35.701	5.19	0.063
f (mm/rev)	1	92.952	92.952	13.52	0.010
Error	6	41.238	6.873		
Total	11	215.061			
Fy					
Vc (m/min)	1	1.08	1.08	0.27	0.622
f (mm/rev)	1	620.366	620.366	155.01	0.000
Error	6	24.013	4.002		
Total	11	651.771			
Fz					
Vc (m/min)	1	0.7021	0.7021	0.12	0.738
f (mm/rev)	1	14.4747	14.4747	2.54	0.162
Error	6	34.1742	5.6957		
Total	11	64.0145			
R					
Vc (m/min)	1	8.338	8.338	1.14	0.327
f (mm/rev)	1	529.093	529.093	72.28	0.000
Error	6	43.919	7.32		
Total	11	644.338			

architecture. Consequently, anisotropy associated with FFF layer orientation was not treated as an independent variable.

Nevertheless, interlayer bonding quality and raster orientation may affect local machinability, particularly with respect to chip formation and subsurface integrity. The trends observed in cutting forces and temperature should therefore be interpreted as specific to the selected build configuration. Further work is required to systematically quantify the effect of build orientation on the machining response of FFF manufactured PLA.

The present study focuses on the machinability of a single thermoplastic material, namely PLA manufactured by fused filament fabrication, using one cutting tool geometry under dry and compressed-air-assisted turning conditions. This scope was deliberately selected to isolate the fundamental thermomechanical behaviour of FFF-fabricated PLA and to minimise confounding effects associated with tool material, coating, or coolant variability. As a result, the findings should be interpreted within this defined experimental framework. The influence of alternative polymer systems, different cutting tool materials or geometries, and liquid-based cooling or lubrication strategies falls outside the scope of this work and represents a relevant direction for future investigations.

4 Conclusions

The feasibility of machining parts obtained by FFF additive manufacturing has been studied to improve the final product quality. The machinability of a PLA thermoplastic material has been evaluated to establish a relationship between cutting parameters and output variables such as maximum machining temperature, cutting forces, active energy consumption, and active power for each experimental trial.

The importance of using external compressed air as an external cooling element has been demonstrated. Under not cooling conditions, thermoplastic chips re-adhere to the newly machined surface due to cutting temperature, worsening the final product quality.

The influence of compressed air reduces the maximum process temperature and facilitates chip evacuation, resulting in superior final quality. The maximum cutting temperature is a critical factor, as it can exceed the glass transition temperature of PLA.

In summary, feed rate primarily governs the mechanical response and the resulting surface quality, whereas cutting speed controls the thermal and power related behaviour. Both effects should be considered when defining post processing strategies for FFF manufactured PLA.

The influence of feed rate was confirmed. Increasing feed rate reduces the time of tool material interaction and the

relative contribution of frictional contact per unit length of cut. This is associated with lower process temperatures and shorter cycle times, while maintaining a more homogeneous surface under stable cutting conditions.

Cutting speed exhibited statistically significant effects on temperature and energy related metrics. By contrast, its influence on the force components was not statistically significant within the investigated range and is therefore treated as a secondary effect in the discussion.

In terms of surface quality, the effectiveness of lathe machining on parts obtained by FFF additive manufacturing has been evaluated. Two surfaces printed with layer heights of 0.30 mm and 0.05 mm have been established. Compared to the surface corresponding to a layer height of 0.30 mm, all machining trials have improved the surface quality of the cylindrical product in terms of *Ra*, *Rz*, and *Rq*.

Regarding specimens obtained with a layer height of 0.05 mm, better surface qualities have been obtained only by increasing the feed rate between 0.15 mm/rev and 0.20 mm/rev. This demonstrates the effectiveness of lathe machining as a secondary operation against high quality additive manufacturing FFF process. This has allowed for better results, improved thermoplastic material behavior, and a considerable reduction in production times.

Beyond confirming known trends in thermoplastic machining, this study contributes a comprehensive and application-oriented evaluation of the machinability of FFF manufactured PLA, linking thermal behaviour, mechanical response, energy consumption, and surface quality within a single experimental framework. The results support the use of turning as an efficient post processing operation for additively manufactured PLA components, particularly in rotational geometries where productivity and surface integrity are critical.

In addition to corroborating general trends previously reported for thermoplastic machining, this study provides an integrated machinability characterisation for FFF manufactured PLA, relating thermal response, mechanical loading, energy demand, and surface finish within a single experimental framework. From an industrial standpoint, the findings indicate that compressed air assisted turning can serve as an efficient and repeatable post processing step for rotational FFF parts. It enables improved surface quality and may reduce overall production time relative to fine layer printing strategies by shifting surface finish requirements from the printing stage to a controlled finishing operation. From an industrial viewpoint, hybrid routes are increasingly motivated by the need for cost-effective and efficient manufacturing solutions, as discussed in broader manufacturing contexts [50].

Author contributions Developed machining tests: F.B.; Data treatment: F.B., F.J.T, S.M.B; Bibliographic search: F.B.,C.B; Conclusions of the work: F.B., L.S, F.J.T; Analysis of the influence of parameters: F.B., S.M.B; Writing the original manuscript and tables: F.B., C.B., S.M.B; Figure elaboration: F.B., F.J.T, S.M.B, C.B.; Manuscript and grammar review: F.J.T, L.S; Critical comments on the final manuscript: S.M.B, F.J.T, C.B., L.S. The authors read and approved the final manuscript.

Funding Funding for open access publishing: Universidad de Málaga/CBUA. Funding for open access charge: Universidad de Málaga / CBUA

Data availability No datasets were generated or analysed during the current study.

Declarations

Conflict of interest The authors declare no conflict of interest.

Ethical approval Not applicable.

References

1. Liu M, Yi H, Cao H (2023) Additive Manufacturing (AM) for advanced materials and structures: green and intelligent development trend. Crystals (Basel) 13:92. https://doi.org/10.3390/cryst13010092
2. Khorasani M, Ghasemi AH, Rolfe B, Gibson I (2022) Additive manufacturing a powerful tool for the aerospace industry. Rapid Prototyp J 28:87–100. https://doi.org/10.1108/RPJ-01-2021-0009
3. Gotkhindikar N, Mehta P, Londhe S et al (2022) A novel FDM based additive manufacturing of PLA components using optimized deep learning strategy. Int J Res Appl Sci Eng Technol 10:1042–1049. https://doi.org/10.22214/ijraset.2022.41436
4. Cao L, Xiao J, Kim JK, Zhang X (2023) Effect of post-process treatments on mechanical properties and surface characteristics of 3D printed short glass fiber reinforced PLA/TPU using the FDM process. CIRP J Manuf Sci Technol 41:135–143. https://doi.org/10.1016/j.cirpj.2022.12.008
5. Hashmi AW, Mali HS, Meena A (2021) The surface quality improvement methods for FDM printed parts: a review. Fused Depos Model Based 3D Print pp 167–194
6. Baechle-Clayton M, Loos E, Taheri M, Taheri H (2022) Failures and flaws in fused deposition modeling (FDM) additively manufactured polymers and composites. J Compos Sci 6(7):202
7. Deb D, Jafferson JM (2021) Natural fibers reinforced FDM 3D printing filaments. In: materials today: proceedings. Elsevier Ltd, pp 1308–1318

8. Finnes T, Letcher T (2015) High definition 3D printing-comparing. SLA and FDM Printing Technologies
9. Al-Ghamdi KA (2019) Sustainable FDM additive manufacturing of ABS components with emphasis on energy minimized and time efficient lightweight construction. Int J Lightweight Mater Manuf 2:338–345. https://doi.org/10.1016/j.ijlmm.2019.05.004
10. Dey A, Yodo N (2019) A systematic survey of FDM process parameter optimization and their influence on part characteristics. J Manuf Mater Process 3(3):64
11. Park SJ, Lee JE, Park JH et al (2020) Enhanced solubility of the support in an FDM-based 3D printed structure using hydrogen peroxide under ultrasonication. Adv Mater Sci Eng 2018(1):3018761. https://doi.org/10.1155/2018/3018761
12. Didier P, Le Coz G, Robin G et al (2022) Consideration of additive manufacturing supports for post-processing by end milling: a hybrid analytical–numerical model and experimental validation. Progress Additive Manuf 7:15–27. https://doi.org/10.1007/s40964-021-00211-4
13. Parvez MM, Patel S, Isanaka SP, Liou F (2021) A novel laser-aided machining and polishing process for additive manufacturing materials with multiple endmill emulating scan patterns. Appl Sci (Switzerland) 11(20):9428. https://doi.org/10.3390/app11209428
14. Grigoriev S, Metel A, Volosova M et al (2022) Combined treatment of parts produced by additive manufacturing methods for improving the surface quality. Technologies (Basel) 10(6):130. https://doi.org/10.3390/technologies10060130
15. Nguyen TK, Lee BK (2018) Post-processing of FDM parts to improve surface and thermal properties. Rapid Prototyp J 24:1091–1100. https://doi.org/10.1108/RPJ-12-2016-0207
16. Jin Y, Wan Y, Liu Z (2017) Surface polish of PLA parts in FDM using dichloromethane vapour. MATEC Web of Conferences 95:05001. https://doi.org/10.1051/matecconf/20179505001
17. Tiwary VK, Arunkumar P, Deshpande AS, Rangaswamy N (2019) Surface enhancement of FDM patterns to be used in rapid investment casting for making medical implants. Rapid Prototyp J 25:904–914. https://doi.org/10.1108/RPJ-07-2018-0176
18. Levenhagen NP, Dadmun MD (2019) Improving Interlayer Adhesion in 3D printing with surface segregating additives: improving the isotropy of acrylonitrile-butadiene-styrene parts. ACS Appl Polym Mater 1:876–884. https://doi.org/10.1021/acsapm.9b00051
19. Wang J, Hu S, Yang B et al (2022) Novel three-dimensional-printing strategy based on dynamic urea bonds for isotropy and mechanical robustness of large-scale printed products. ACS Appl Mater Interfaces 14:1994–2005. https://doi.org/10.1021/acsami.1c20659
20. Ravi AK, Deshpande A, Hsu KH (2016) An in-process laser localized pre-deposition heating approach to inter-layer bond strengthening in extrusion based polymer additive manufacturing. J Manuf Process 24:179–185. https://doi.org/10.1016/j.jmapro.2016.08.007
21. Nsengimana J, Van der Walt J, Pei E, Miah M (2019) Effect of post-processing on the dimensional accuracy of small plastic additive manufactured parts. Rapid Prototyp J 25:1–12. https://doi.org/10.1108/RPJ-09-2016-0153
22. Yan Y, Mao Y, Li B, Zhou P (2020) Machinability of the thermoplastic polymers: PEEK, PI, and PMMA. Polymers (Basel) 13:69. https://doi.org/10.3390/polym13010069
23. Xiao KQ, Zhang LC (2002) The role of viscous deformation in the machining of polymers. Int J Mech Sci 44:2317–2336. https://doi.org/10.1016/S0020-7403(02)00178-9
24. Kousiatza C, Chatzidai N, Karalekas D (2017) Temperature mapping of 3D printed polymer plates: experimental and numerical study. Sensors (Switzerland) 17(3):456. https://doi.org/10.3390/s17030456
25. Masek P, Zeman P, Kolar P Cutting temperature measurement in turning of thermoplastic composites using a tool-work thermocouple. Int J Adv Manuf Technol 116(9):3163-3178. https://doi.org/10.1007/s00170-021-07588-0/Published
26. Somireddy M, Czekanski A (2021) Computational modeling of constitutive behaviour of 3D printed composite structures. J Mater Res Technol 11:1710–1718. https://doi.org/10.1016/j.jmrt.2021.02.030
27. Hocheng H, Tsao CC (2005) The path towards delamination-free drilling of composite materials. J Mater Process Technol 167:251–264. https://doi.org/10.1016/j.jmatprotec.2005.06.039
28. Aruna M (2020) Optimization of cutting parameters in machining polyoxymethylene using RSM. In: IOP Conference Series: Materials Science and Engineering. IOP Publishing Ltd
29. Erenkov OYu, Yavorskii DO, Kalenskii AM, Lopushanskii IY (2020) Turning of thermoplastics using ceramic cutting tools. Glass Ceram 77:194–196. https://doi.org/10.1007/s10717-020-00268-7
30. Syrlybayev D, Seisekulova A, Talamona D, Perveen A (2022) The post-processing of additive manufactured polymeric and metallic parts. J Manuf Mater Process 6:116. https://doi.org/10.3390/jmmp6050116
31. Lavecchia F, Guerra MG, Galantucci LM (2022) Chemical vapor treatment to improve surface finish of 3D printed polylactic acid (PLA) parts realized by fused filament fabrication. Progress Additive Manuf 7:65–75. https://doi.org/10.1007/s40964-021-00213-2
32. Chueca de Bruijn A, Gómez-Gras G, Pérez MA (2021) On the effect upon the surface finish and mechanical performance of ball burnishing process on fused filament fabricated parts. Addit Manuf 46:102133. https://doi.org/10.1016/j.addma.2021.102133
33. Baron JD, Naveed MO, Chen L (2025) An experimental investigation of hybrid fused filament fabrication with in-process machining. Manuf Lett 44:442–452. https://doi.org/10.1016/j.mfglet.2025.06.053
34. Boschetto A, Bottini L, Veniali F (2016) Finishing of fused deposition modeling parts by CNC machining. Robot Comput Integr Manuf 41:92–101. https://doi.org/10.1016/j.rcim.2016.03.004
35. Alzyod H, Konya G, Ficzere P (2025) Maximizing material removal rate and surface smoothness in MEX parts through turning process optimization using BBD. Progress Additive Manuf 10:10295–10309. https://doi.org/10.1007/s40964-025-01241-y
36. Patil AS, Sunnapwar VK, Bhole KS et al (2026) Surface texture evaluation in turning of Ti6Al4V under nano-flood cooling environment. pp 1–8
37. Patil A, Sunnapwar V, Bhole K et al (2024) Investigation of open pocket 3D milling of Ti6Al4V by grey relational approach. pp 020006
38. Decker C (2000) Photocrosslinking of functionalized rubbers IX. Thiol-ene polymerization of styrene-butadiene-block-copolymers. Polymers (Guildf) 41:3905–3912. https://doi.org/10.1016/S0032-3861(99)00649-7
39. Bareggi A, O'Donnell GE (2015) Thermal and mechanical effects of high-speed impinging jet in orthogonal machining operations: experimental, finite elements and analytical investigations. Proc Inst Mech Eng B J Eng Manuf 229:379–391. https://doi.org/10.1177/0954405414530897
40. Chang DY, Lin CH, Wu XY et al (2023) Cutting force, vibration, and temperature in drilling on a thermoplastic material of PEEK. J Thermoplast Compos Mater 36:1088–1112. https://doi.org/10.1177/08927057211052325
41. Li R, Zhang Z, Fang T (2016) Experimental research on swelling and glass transition behavior of poly(methyl methacrylate) in supercritical carbon dioxide. J Supercrit Fluids 110:110–116. https://doi.org/10.1016/j.supflu.2015.12.017

42. Xu W, Zhang L (2019) Heat effect on the material removal in the machining of fibre-reinforced polymer composites. Int J Mach Tools Manuf 140:1–11. https://doi.org/10.1016/j.ijmachtools.2019.01.005
43. Mohan NS, Ramachandra A, Kulkarni SM (2005) Machining of fiber-reinforced thermoplastics: influence of feed and drill size on thrust force and torque during drilling. J Reinf Plast Compos 24:1247–1257. https://doi.org/10.1177/0731684405049865
44. Zhang D, Zhang XM, Nie GC et al (2021) Characterization of material strain and thermal softening effects in the cutting process. Int J Mach Tools Manuf 160:103672. https://doi.org/10.1016/j.ijmachtools.2020.103672
45. Wcisło B (2016) Simulations of thermal softening in large strain thermoplasticity. Eng Trans 64
46. Bintara RD, Lubis DZ, Aji Pradana YR (2021) The effect of layer height on the surface roughness in 3D printed polylactic acid (PLA) using FDM 3D printing. IOP Conf Ser Mater Sci Eng 1034:012096. https://doi.org/10.1088/1757-899x/1034/1/012096
47. Kočiško M, Štafura L, Goryl K, Mitaľová Z (2025) Evaluation of the effect of post-processing methods on the surface parameters of parts produced by FFF/FDM technology. Materials 18:4672. https://doi.org/10.3390/ma18204672
48. Mathew A, Kishore SR, Tomy AT et al (2023) Vapour polishing of fused deposition modelling (FDM) parts: a critical review of different techniques, and subsequent surface finish and mechanical properties of the post-processed 3D-printed parts. Progress Additive Manuf 8:1161–1178. https://doi.org/10.1007/s40964-022-00391-7
49. Carta M, Loi G, El Mehtedi M et al (2025) Improving surface roughness of FDM-printed parts through CNC machining: a brief review. J Compos Sci 9:296. https://doi.org/10.3390/jcs9060296
50. Shinde SM, Lekurwale RR, Bhole KS et al (2022) On efficient electrode design and manufacturing techniques for hot die steel inserts. Int J Interact Des Manuf (IJIDeM). https://doi.org/10.1007/s12008-022-00994-y